Distorting the top resonance with effective interactions

Felix Egle,[1,*] Christoph Englert,[2,†] Margarete Mühlleitner,[3,‡] and Michael Spannowsky[4,§]
[1]*Deutsches Elektronen-Synchrotron DESY, Notkestraße 85, 22607 Hamburg, Germany*
[2]*Department of Physics & Astronomy, University of Manchester, Manchester M13 9PL, United Kingdom*
[3]*Institute for Theoretical Physics, Karlsruhe Institute of Technology, 76128 Karlsruhe, Germany*
[4]*Institute for Particle Physics Phenomenology, Department of Physics, Durham University, Durham DH1 3LE, United Kingdom*

(Received 9 May 2025; accepted 31 October 2025; published 1 December 2025)

Interference effects in effective field theory (EFT) analyses can significantly distort sensitivity expectations, leaving subtle yet distinct signatures in the reconstruction of final states crucial for limit setting around Standard Model predictions. Using the specific example of four-fermion operators in top-quark pair production at the Large Hadron Collider (LHC), we provide a detailed quantitative assessment of these resonance distortions. We explore how continuum four-fermion interactions affect the resonance shapes, creating potential tensions between the high-statistics resonance regions and rare, high momentum-transfer continuum excesses. Our findings indicate that, although four-fermion interactions do modify the on-shell region comparably to continuum enhancements, current experimental strategies at the high-luminosity LHC are unlikely to capture these subtle interference-induced distortions. Nonetheless, such effects could become critical for precision analyses at future lepton colliders, such as the FCC-ee. Our work underscores the importance of resonance-shape measurements as complementary probes in global EFT approaches, guiding robust and self-consistent experimental strategies in ongoing and future high-energy physics programs.

DOI: 10.1103/2rz1-55f5

I. INTRODUCTION

Effective field theory (EFT) [1,2] is increasingly becoming the new standard for framing the sensitivity to new physics interactions under well-defined theoretical assumptions. From the first proof-of-principle analyses, this has evolved into a cohesive program spanning many different processes to obtain a global picture, including efforts by the experiments directly. Many approaches to setting constraints on process-relevant interactions rely on a good knowledge of relevant Standard Model (SM) correlations to extract the SM null hypothesis used for setting limits.

When considering EFT deformations of the SM, this issue is further highlighted by the presence of nonresonant, non-SM contributions, which can lead to interference-related distortions of SM particle thresholds, e.g., through changing the line profile of intermediate unstable particles such as the top quark or the W boson when reconstructed from their decay products. This can implicitly affect any EFT analysis at the Large Hadron Collider (LHC) and future facilities and needs to be contrasted with direct beyond the Standard Model (BSM)-related modifications of the particles' resonance shapes directly.

Turning to analyses of top final states [3–8], the relevance (and limitations) of top-pole measurements are well documented in the literature. In the SM, nonperturbative effects [9,10] are known to create systematic complications in extracting the top quark mass, chiefly from the analysis of top pair final states with a large abundance at the LHC. When turning to EFT modifications and, importantly, to new irreducible contributions to the amplitude of these final states, interference effects can enter the $pp \to \bar{t}t$ alongside the top quark decay. More concretely, the extraction of the top threshold that fundamentally underpins any signal-vs-background analysis of a $t\bar{t}$ system may be impacted by the presence of new physics contributions, e.g., by how much contact interactions in the vicinity of the W threshold sculpt the kinematic correlations used to "tag" the top quark. Concretely, the squared SM-like matrix element in the vicinity of a resonance is well described for widths $\Gamma \ll m$ by a Breit-Wigner distribution,

*Contact author: felix.egle@desy.de
†Contact author: christoph.englert@manchester.ac.uk
‡Contact author: margarete.muehlleitner@kit.edu
§Contact author: michael.spannowsky@durham.ac.uk

Published by the American Physical Society under the terms of the Creative Commons Attribution 4.0 International license. Further distribution of this work must maintain attribution to the author(s) and the published article's title, journal citation, and DOI. Funded by SCOAP³.

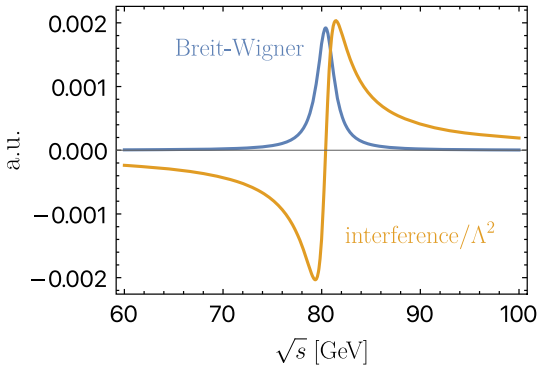

FIG. 1. Representative normalized Breit-Wigner distribution for the W mass of $(m_W, \Gamma_W) \approx (80.4, 2.08)$ GeV. The Breit-Wigner distribution is normalized to unity. In this plot, it can be considered as the scale for the overall peak cross section observed in a scattering experiment. The interference effect is given as const $\times$ 2Re$[\mathcal{M}]/16\pi^2$. The Breit-Wigner suppression of the differential cross section can therefore be comparable with a loop suppression assumed to be constant here. The effect will quickly decouple $\sim\Lambda^{-2}$, and we investigate these interference effects for a realistic interaction in Sec. III.

$$\mathcal{M}_{\mathrm{SM}} \underset{s\simeq m^2}{\simeq} \frac{1}{s - m^2 + i\Gamma m}, \tag{1}$$

in the vicinity of the resonance mass for a relevant kinematic distribution s. Any additional, approximately constant contribution $\mathcal{M}_{\mathrm{BSM}}$ for $s \simeq m^2$ therefore "tilts" the Breit-Wigner at interference level $\mathrm{d}\sigma \sim 2\mathrm{Re}(\mathcal{M}_{\mathrm{SM}}\mathcal{M}^*_{\mathrm{BSM}})$. In doing so, the Breit-Wigner suppression can be numerically mitigated. More concretely, dimension-six effects $\sim 1/\Lambda^2$ that have a flat behavior across the resonance peak are magnified by the resonance structure leading to the characteristic behavior displayed in Fig. 1. While the SM amplitude scales with the modulus of the Breit-Wigner propagator $|D(p^2)|^2$ Eq. (1) (cf. also the narrow-width approximation), the interference scales $\sim$const $\times\, D(p)/\Lambda^2$, i.e., the contribution decouples less quickly off resonance. However, the interference will decouple proportional to the SM width and the mass scale of the BSM theory Λ.[1] The fact that such interference effects can severely impact and limit the experimental sensitivity to new physics is well established in searches for exotic Higgs bosons [13–16], which drives experimental searches, cf., e.g., [17].

A phenomenologically relevant question therefore arises: Can effective contributions affect the reconstruction of SM candles which are used to set constraints on these interactions in the first place? If the answer to this question were yes, such modifications would enable a *process-specific* test for new physics from reconstructed SM particle thresholds at the price of increased experimental complexity in defining the SM null hypothesis. A sizable effect could also, in part, address the anomalous measurement of the W mass as observed by the CDF collaboration [18]. The net effect of the interference displayed alongside the Breit-Wigner shape in Fig. 1 can be understood as a shift of the resonance peak location, depending on the size of the EFT contribution and its sign. These effects are probed in threshold observables which are sensitive to the production mechanism, i.e., the sampled invariant mass distribution, as different shapes at pp colliders compared to $p\bar{p}$ colliders. Of course, any such indication would require confirmation from D0. More generally, such observations could open up new possibilities for searches of new physics at future precision facilities, such as the FCC-ee.

Of course, any such new contribution might also be visible in the tails as a function of s. In the case of, e.g., four-fermion interactions, these effects are even kinematically enhanced. Therefore, it is not clear whether the limit setting from distribution tails is already constraining enough to render on-shell modifications (beyond total width and, hence, branching ratio fits) relevant. This paper aims to reach a quantitative estimate of these effects within the SMEFT framework [19]. We focus on the $t\bar{t}$ final state as it is one of the most abundant processes at the LHC and, therefore, prone to provide good *a priori* sensitivity to SMEFT relevant deformations. We organize this work as follows: In Sec. II, we provide a short overview of our analysis setup before we consider representative effects in detail in Sec. III. Section IV provides a summary and conclusions with a positive message for the experimental community: We gather evidence that within the limits observed from tails, no significant on-shell distortion is observed. Current approaches can therefore be considered self-consistent and robust.

II. ELEMENTS OF THE ANALYSIS

In this study, we use the SMEFT framework at dimension six [19],

$$\mathcal{L} = \mathcal{L}_{\mathrm{SM}} + \sum_i \frac{c_i}{\Lambda^2} O_i, \tag{2}$$

where O_i denote the dimension-six operators and Λ the new physics scale, to investigate the influence of new physics on top quark pair production at the LHC. In our analysis, we isolate the contributions from new EFT physics by adjusting the Wilson coefficients c_i. For the generation of our event samples, we employ MADGRAPH_AMC@NLO [20] together with SMEFTSIM3.0.2 [21]. In practice, we generate around two million events for the SM as well as one million events for the EFT operator interference (we comment on the so-called quadratic dimension-six effects below), which is enough statistics for a smooth extrapolation to the high-luminosity

[1]Such effects have been discussed in the literature in the SM (for a recent review, see, e.g., [11,12] including discussions of scheme dependencies).

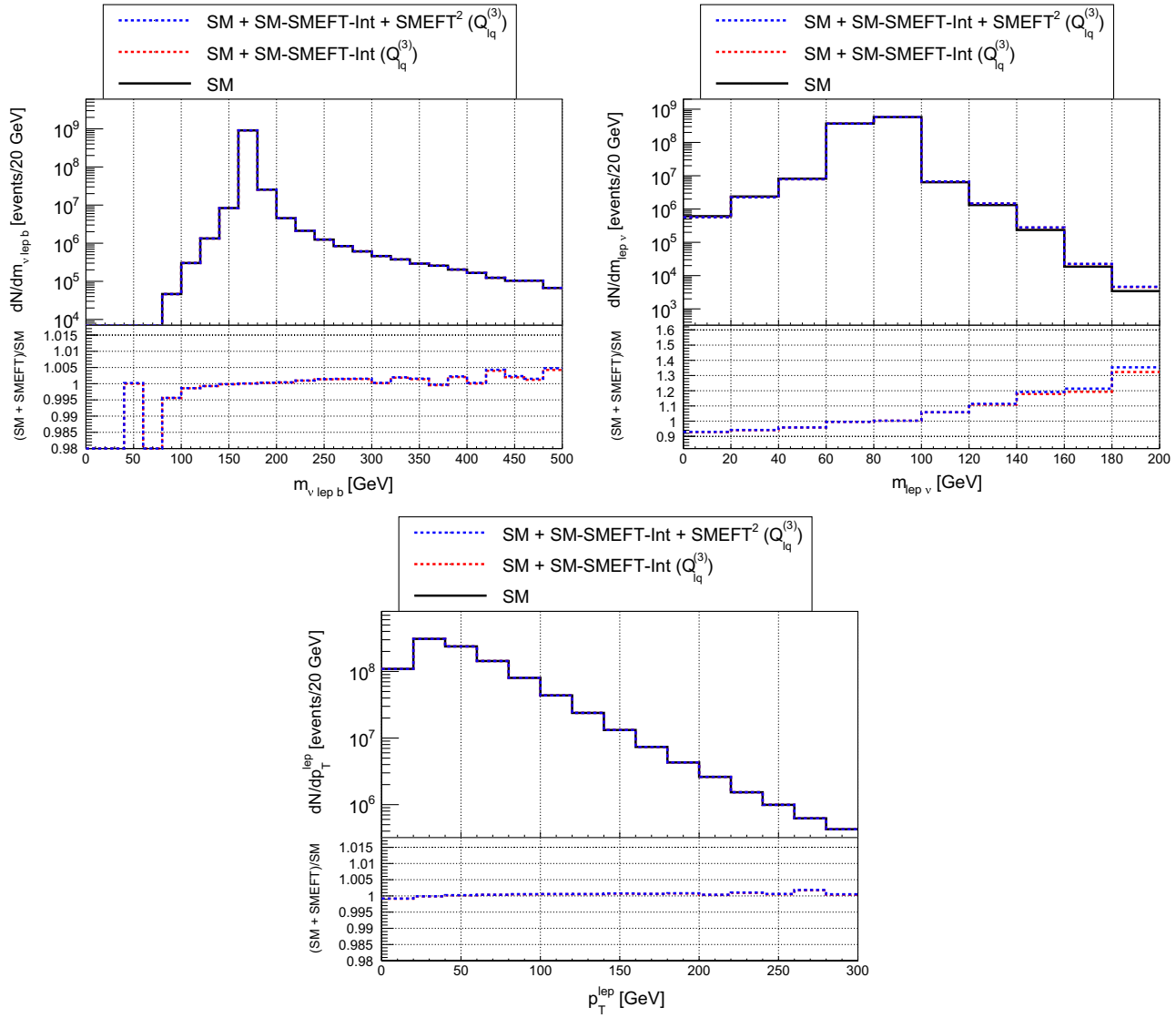

FIG. 2. Energy-transfer sensitive differential distributions of semileptonic $t\bar{t}$ LHC production with *a priori* sensitivity to the new interactions discussed in this work, here specifically for the operator $O_{lq}^{(3)}$ (with strength $1/\mathrm{TeV}^2$) for illustration purposes. Particularly relevant to the focus of this work are the invariant mass distributions, which are sensitive to resonance distortion. Hence, we show the invariant neutrino-lepton, and neutrino-lepton-bottom quark invariant masses, but also the lepton transverse momentum p_T^{lep} for comparison with a luminosity of $\mathcal{L} = 3\ \mathrm{ab}^{-1}$. The lower insets show the ratio of BSM distributions (either at dimension-six level or including squared dimension-six contributions) with respect to the SM.

phase of the LHC (3/ab) whilst capturing subtle deviations with sufficient statistics.

To highlight the on-shell/off-shell interplay alluded to above, we focus first on the operators,

$$Q_{lq}^{(3)} = (\bar{l}\gamma_\mu \tau^I l_R)(\bar{q}_3 \gamma^\mu \tau^I q_3), \tag{3}$$

which can interfere with the top decay mediated by the W boson in the SM. As the W boson decays on shell, the $Q^{(3)}$-interference term distorts the shape of the W resonance that, in turn, is used in generic reconstruction techniques for the top quark [22].

In this paper, we do not attempt to establish a global picture of top-quark interactions but note that the new physics operators used here as a "strawman" scenario are also relevant in flavor physics, see, e.g., [6,23–25].

We analyze a range of differential distributions, such as the transverse momentum (p_T) for each final state particle and various invariant mass systems linked to the top-quark decay. We conservatively take bin sizes of 20 GeV and focus on fully and semileptonic top decays from $pp \to t\bar{t}$ collisions at 13 TeV. The selection of different bin sizes allows us to study the results' sensitivity to the data's granularity when considering the impact of the aforementioned interference effects. To quantify the deviations from

the Standard Model predictions, we performed a χ^2 test, defined as

$$\chi^2 = \sum_i^{\#\text{bins}} \frac{(N_{i,\text{SM+SMEFT}} - N_{i,\text{SM}})^2}{\sigma^2_{i,\text{SM+SMEFT}} + \sigma^2_{i,\text{SM}}}, \tag{4}$$

where σ_i is the error on a bin count $N_i = \sigma_i \times \mathcal{L}$, given by $\sqrt{N_i}$ (we comment on the impact of systematic uncertainties below, but ignore theoretical uncertainties and will come back to this in the conclusions). This method allows us to assess the goodness of fit between the SM predictions and the observed data, including potential contributions from new physics. To evaluate the critical threshold above which the SM null hypothesis will be rejected (and to compute 95% confidence level limits depending on the degrees of freedom relevant to the specific distribution under investigation), we employ a bisection method to find the limits for the Wilson coefficients, which iteratively adjusts the coefficients to find the point where the observed χ^2 exceeds the critical value (determined by the number of bins and confidence level).

Of course, four-fermion interactions involving a single top quark are already constrained from top width measurements, i.e., fits to the top quark's branching ratios, but also flavor physics measurements [6,24,25]. To reflect the measurements directly relevant to our analysis [23,26], we include the top width measurement of $\Gamma_t = 1.34 \pm 0.16$ GeV [27] as an additional contribution to the χ^2 test statistic. To gain a quantitative understanding of how operators can lead to on-shell distortion in tension against constraints from continuum enhancement, we compare the limits of two different exclusive phase space regions:

(a) the "on-shell (OS) region" related to the top and W thresholds, respectively. We include all bins around the t and W thresholds in the corresponding invariant mass distributions that are in the region $[m_t - 2\Gamma_t, m_t + 2\Gamma_t]$ and $[m_W - 2\Gamma_W, m_W + 2\Gamma_W]$.
(b) the "off-shell region" that complements the on-shell regions as defined above; in particular, these contain the tails of the distributions susceptible to EFT continuum modifications. More precisely, this selects the tail region, only considering bins beyond the OS region.

We include these regions and the limits on the Wilson coefficients derived from these quantities only for the invariant mass distributions with a top quark or a W boson threshold. The interference-related histograms for $O_{lq}^{(3)}$ are shown in Fig. 2, for momentum-dependent distributions that are used both for the reconstruction of the signal process and the new physics limit setting, see, e.g., [22].

III. RELEVANCE OF RESONANCE DISTORTION FROM A TOY FIT

Any significant distortion of the involved resonance structures already at the Monte Carlo truth indicates a significant *a priori* issue for experimental analyses. From Fig. 2 it is immediately obvious that not all observables are equally suited to set strong constraints on the presence of new physics even when they are correlated. For instance, for the contact interaction that is related to the leptonic top decay, there are cancellations in the reconstructed top mass. A similar feature can be observed for the W threshold. The behavior of the $l\nu$ system (we denote $m_{\text{lep}\nu}$ as the truth-level invariant lepton-neutrino mass that is approximated by experimental reconstruction) below and above the top threshold is exactly the behavior motivated in Fig. 1, coarse grained to the bin size of 20 GeV that we consider in this work (this seems a conservative choice in the light of Ref. [28] and the data improvement that we can expect at the high-luminosity LHC phase).

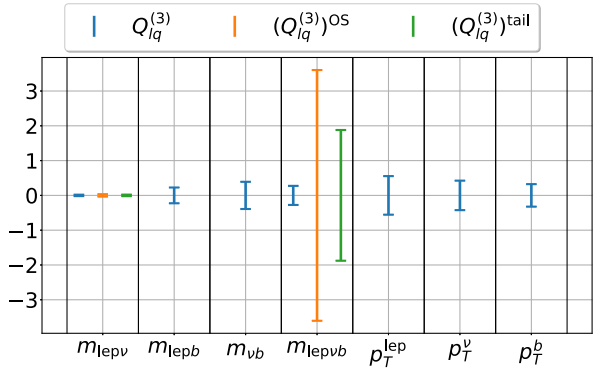

FIG. 3. HL-LHC constraints on the four-fermion interactions discussed in this work for $\Lambda = 1$ TeV, including a comparison of the single discriminants for the limit setting. When considering on-shell and tail distributions, the different constraints are highlighted in orange and green, respectively. No systematics are included in this comparison; for additional details, see the main body of the text.

As expected from contact interactions, all invariant masses are enhanced above the respective particle thresholds. However, the kinematics is modified through redistributing the recoil in such a way that the lepton transverse momentum remains comparably unchanged, see Fig. 2. The recoil is redistributed between the b and neutrino system by the four-fermion interaction. Such an effect is suppressed for the W exchange that determines the kinematical correlations expected for the SM contribution. Together, therefore, the reconstructed W system yields the most significant relative modification. This will then be reflected in a comparably tighter limit that can be achieved from this observable compared to the other observables in Fig. 2: The result of the described limit-setting exercise is shown in Fig. 3.[2] Here, we also show limits for the tail and OS region where those have been defined (cf. Sec. II). Specifically, these are the invariant mass distributions of the

[2]We report limits in this work obtained using the linearized dimension-six contributions. However, we have cross-checked quadratic effects and find consistent results.

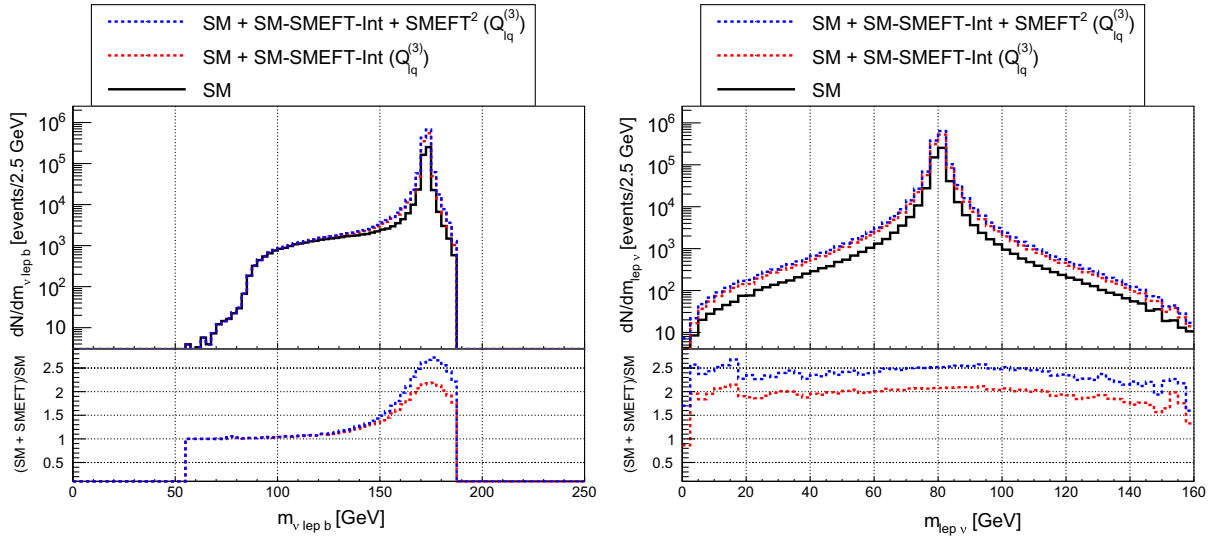

FIG. 4. W line shape–related observables (again with strength $1/\mathrm{TeV}^2$ for illustration) with *a priori* sensitivity to resonance distortion for e^+e^- collisions running close to the $t\bar{t}$ threshold with a luminosity of $\mathcal{L} = 2.65\ \mathrm{ab}^{-1}$. The shape change of the distributions relative to the SM is more pronounced than at hadron colliders, indicating a greater intrinsic sensitivity at the FCC-ee.

particles originating from the top quark or the W boson, respectively, where we can separate the OS region around the top and W boson thresholds from the tails region above the respective particle thresholds.

Of course, systematics can further impact the quality of the limit extraction. If they are included as a fractional contribution related to the bin entries in Eq. (4), e.g., the limit on $Q_{lq}^{(3)}$ from the p_{T}^b distribution changes from $[-0.323, 0.323]$ to $[-0.404, 0.404]$ for a (conservative) systematic uncertainty of 25% ($\Lambda = 1$ TeV). Similarly, the limit on $Q_{lq}^{(3)}$ using the $m_{\mathrm{lep}\nu}$ distribution changes from $[-0.021, 0.021]$ to $[-0.026, 0.026]$. The discrepancy between different observables is directly related to their response to the particular interaction studied here. As can be seen in Fig. 2, the invariant lepton-neutrino mass exhibits a larger shape deviation across the resonance threshold, which is diluted through its integrated effect in other observables.

With these results at hand, we can conclude that resonance distortion is not a relevant effect in the hadron collider environment, and the SM reconstruction techniques remain robust: Both the OS and the nonresonant region might provide comparable statistical sensitivity with interference effects present, but the coarse graining of measured invariant mass distributions mitigates distortion effects leaving only a slight asymmetry as visible in Fig. 2. This still could leave them relevant for unbinned approaches; we encourage the LHC experiments to include self-consistency checks along the lines of the discussion in this paper.

In collider environments that enable a more detailed exploration of the top pair threshold, this could, in principle, be different. A potential FCC-ee, which is under active consideration as part of the current ECFA process, could feature a top quark pair production program at a c.m. energy of $\sqrt{s} = 350$–365 GeV, collecting a luminosity of around $1.8 \times 10^4\ \mathrm{fb}^{-1}$ per year. To gain a quantitative estimate of the relevance of the effects discussed in the work in such an environment, we reperform the above limit setting analysis for $e^+e^- \to t\bar{t}$, running at the top pair threshold (see also [29–33] and the BSM studies of [34–38]). More concretely, we consider a center-of-mass energy of 2×180 GeV and a luminosity of $\mathcal{L} = 2.65\ \mathrm{ab}^{-1}$ [39].[3]

Comparing results to the high-luminosity LHC (HL-LHC) environment, we again observe a slight asymmetry of the reconstructed W mass in $t\bar{t}$ final states, see Figs. 4 and 5. (Similar to Fig. 3, we include a comparison of OS and off-shell regions where particle thresholds are accessible according to the definition of Sec. II.) The precision environment of a lepton collider enables more fine-grained measurements, and we opt for a 2.5 GeV binning.

The limit from the $m_{\mathrm{lep}\nu}$ distribution considering only the OS region for $Q_{lq}^{(3)}$ is $[-0.0059, 0.0059]$ (decreasing to $[-0.0074, 0.0074]$ for a flat 25% systematic uncertainty); from the p_{T}^b distribution we obtain $[-0.015, 0.015]$ ($[-0.018, 0.018]$). However, it is worth pointing out that these effects are also susceptible to the theoretical uncertainties related to renormalization scheme choices. We can also conclude that a new BSM contribution that remains "flat" across the W boson threshold does not impact the W reconstruction critically in the particular example of $t\bar{t}$ production at a lepton collider, once more information (i.e., the total rate) is included, cf. Fig. 4.

[3]See also the resources of the FCC-ee Physics Performance Group (https://hep-fcc.github.io/FCCeePhysicsPerformance).

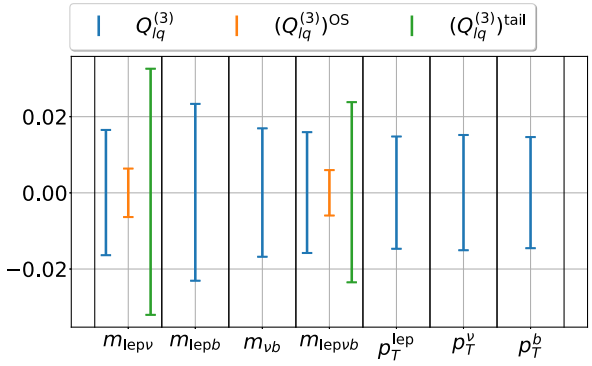

FIG. 5. Limits on $O_{lq}^{(3)}$ (in units $1/\mathrm{TeV}^2$) at an e^+e^- collider running close to the $t\bar{t}$ threshold with an integrated luminosity of $\mathcal{L} = 2.65\ \mathrm{ab}^{-1}$. The impact of systematics is neglected but commented on in the text.

For $e^+e^- \to t\bar{t}$, the top quark kinematics are fixed by the center-of-mass energy, operating close to the $t\bar{t}$ threshold. This is qualitatively different for the LHC, where the top quarks can be produced with large momentum transfers. The invariant mass of the decay products enables a more precise top reconstruction, and the respective invariant mass shows a better limit-setting performance compared to the LHC. This is mostly driven by the rate expectation compared to the SM, which is narrowly clustered around the top threshold. The W decay products are kinematically correlated over a wider phase space and, therefore, their invariant mass has somewhat reduced sensitivity. Therefore, all observables perform similarly in our limit setting exercise as shown in Fig. 5. Where thresholds can be identified according to our definition of Sec. II, the OS region drives the sensitivity relative to the off-shell region, providing the dominant statistical pull in the combination. In comparison with the LHC, this relates to an established phenomenological observation: The discovery potential of hadron machines stems from the wide energy range of pp collisions, whereas e^+e^- machines probe a smaller kinematic window with highest accuracy. Of course, a wider range of interactions than considered here is relevant for an agnostic search for nonresonant physics.

IV. CONCLUSIONS

The study presented here highlights and quantifies the effects of EFT modifications on resonance shapes in top-quark pair production, with a particular emphasis on four-fermion operators within the SMEFT framework. Our detailed investigation of key kinematic distributions relevant to the reconstruction of top-quark events at the high-luminosity LHC reveals subtle interference effects that distort resonance shapes. However, these interference-induced resonance distortions remain negligible due to current collider experimental resolutions and statistical limitations. Thus, existing analysis methodologies at the HL-LHC are robust and are not compromised by the subtle effects explored in this study. Whilst the reported results are based on a linearized treatment of the EFT expansion, we cross-checked "quadratic" effects and find consistency. A more comprehensive inclusion of more realistic fit assumptions, specifically with respect to experimental and theoretical uncertainties that are omitted here, will not change this qualitative picture. We can also expect that the experimental collaborations will further tighten their control over large-momentum transfer regions, which drives the constraints on interactions considered here. This has already been demonstrated in the large improvements in four top final state results (see the discussion in [40]).

Nevertheless, the potential impact of these resonance distortions should not be dismissed outright, particularly in the context of future collider environments offering significantly enhanced sensitivity. For example, resonance distortions can become observable at an electron-positron collider like the FCC-ee, operating near the top-quark production threshold with higher resolution precision elect. Our projections indicate tighter constraints on EFT parameters, i.e., we find a refined sensitivity range of $[-0.0059, 0.0059]$ obtained from analyzing the invariant mass distribution of leptonic W decays at the FCC-ee. This level of sensitivity surpasses what is achievable at the current LHC and shows the value of future precision experiments (see also [41]).

ACKNOWLEDGMENTS

A Leverhulme Trust Research Project Grant No. RPG-2021-031 funds this work. F. E. is supported by the DFG Emmy Noether Grant No. BR 6995/1–1. F. E. acknowledges support by the Deutsche Forschungsgemeinschaft (DFG, German Research Foundation) under Germany's Excellence Strategy—EXC 2121 "Quantum Universe"—390833306. This work has been partially funded by the Deutsche Forschungsgemeinschaft (DFG, German Research Foundation)—491245950. C. E. is supported by the U.K. Science and Technology Facilities Council (STFC) under Grant No. ST/X000605/1 and the Institute for Particle Physics Phenomenology Associateship Scheme. M. M. is supported by the BMBF-Project 05H21VKCCA. M. S. is supported by the STFC under Grant No. ST/P001246/1.

DATA AVAILABILITY

The data are not publicly available. The data are available from the authors upon reasonable request.

[1] S. Weinberg, Physica (Amsterdam) **96A**, 327 (1979).
[2] H. Georgi, Nucl. Phys. **B361**, 339 (1991).
[3] A. Buckley, C. Englert, J. Ferrando, D. J. Miller, L. Moore, M. Russell, and C. D. White, J. High Energy Phys. 04 (2016) 015.
[4] N. P. Hartland, F. Maltoni, E. R. Nocera, J. Rojo, E. Slade, E. Vryonidou, and C. Zhang, J. High Energy Phys. 04 (2019) 100.
[5] I. Brivio, S. Bruggisser, F. Maltoni, R. Moutafis, T. Plehn, E. Vryonidou, S. Westhoff, and C. Zhang, J. High Energy Phys. 02 (2020) 131.
[6] S. Bißmann, C. Grunwald, G. Hiller, and K. Kröninger, J. High Energy Phys. 06 (2021) 010.
[7] J. J. Ethier, G. Magni, F. Maltoni, L. Mantani, E. R. Nocera, J. Rojo, E. Slade, E. Vryonidou, and C. Zhang (SMEFiT Collaboration), J. High Energy Phys. 11 (2021) 089.
[8] F. Garosi, D. Marzocca, A. R. Sánchez, and A. Stanzione, J. High Energy Phys. 12 (2023) 129.
[9] M. Beneke and V. M. Braun, Nucl. Phys. **B426**, 301 (1994).
[10] I. I. Y. Bigi, M. A. Shifman, N. G. Uraltsev, and A. I. Vainshtein, Phys. Rev. D **50**, 2234 (1994).
[11] H. K. Dreiner, H. E. Haber, and S. P. Martin, Phys. Rep. **494**, 1 (2010).
[12] A. Denner and S. Dittmaier, Phys. Rep. **864**, 1 (2020).
[13] K. J. F. Gaemers and F. Hoogeveen, Phys. Lett. **146B**, 347 (1984).
[14] S. Jung, J. Song, and Y. W. Yoon, Phys. Rev. D **92**, 055009 (2015).
[15] B. Hespel, F. Maltoni, and E. Vryonidou, J. High Energy Phys. 10 (2016) 016.
[16] P. Basler, S. Dawson, C. Englert, and M. Mühlleitner, Phys. Rev. D **101**, 015019 (2020).
[17] M. Aaboud *et al.* (ATLAS Collaboration), Phys. Rev. Lett. **119**, 191803 (2017).
[18] T. Aaltonen *et al.* (CDF Collaboration), Science **376**, 170 (2022).
[19] B. Grzadkowski, M. Iskrzynski, M. Misiak, and J. Rosiek, J. High Energy Phys. 10 (2010) 085.
[20] J. Alwall, R. Frederix, S. Frixione, V. Hirschi, F. Maltoni, O. Mattelaer, H. S. Shao, T. Stelzer, P. Torrielli, and M. Zaro, J. High Energy Phys. 07 (2014) 079.
[21] I. Brivio, J. High Energy Phys. 04 (2021) 073.
[22] G. Aad *et al.* (ATLAS Collaboration), J. High Energy Phys. 06 (2022) 063.
[23] M. Chala, J. Santiago, and M. Spannowsky, J. High Energy Phys. 04 (2019) 014.
[24] S. Bißmann, J. Erdmann, C. Grunwald, G. Hiller, and K. Kröninger, Eur. Phys. J. C **80**, 136 (2020).
[25] C. Grunwald, G. Hiller, K. Kröninger, and L. Nollen, J. High Energy Phys. 11 (2023) 110.
[26] O. Atkinson, C. Englert, M. Kirk, and G. Tetlalmatzi-Xolocotzi, Eur. Phys. J. C **85**, 258 (2025).
[27] S. Navas *et al.* (Particle Data Group), Phys. Rev. D **110**, 030001 (2024).
[28] G. Aad *et al.* (ATLAS Collaboration), J. High Energy Phys. 07 (2023) 141.
[29] V. S. Fadin and V. A. Khoze, JETP Lett. **46**, 525 (1987).
[30] A. H. Hoang and T. Teubner, Phys. Rev. D **58**, 114023 (1998).
[31] A. H. Hoang and T. Teubner, Phys. Rev. D **60**, 114027 (1999).
[32] A. H. Hoang, A. V. Manohar, I. W. Stewart, and T. Teubner, Phys. Rev. D **65**, 014014 (2002).
[33] A. Blondel and P. Janot, Eur. Phys. J. Plus **137**, 92 (2022).
[34] P. H. Khiem, E. Kou, Y. Kurihara, and F. Le Diberder, arXiv:1503.04247.
[35] P. Janot, J. High Energy Phys. 04 (2015) 182.
[36] C. Englert and M. Russell, Eur. Phys. J. C **77**, 535 (2017).
[37] R. Jafari, P. Eslami, M. Mohammadi Najafabadi, and H. Khanpour, Phys. Lett. B **806**, 135469 (2020).
[38] J. Ma, S.-Q. Wang, T. Sun, J.-M. Shen, and X.-G. Wu, Chin. Phys. C **48**, 043105 (2024).
[39] H. Abramowicz *et al.* (CLICdp Collaboration), J. High Energy Phys. 11 (2019) 003.
[40] A. Belvedere, C. Englert, R. Kogler, and M. Spannowsky, Eur. Phys. J. C **84**, 715 (2024).
[41] E. Celada, T. Giani, J. ter Hoeve, L. Mantani, J. Rojo, A. N. Rossia, M. O. A. Thomas, and E. Vryonidou, J. High Energy Phys. 09 (2024) 091.